Exploring Ru compatibility with Al-Ge eutectic wafer bonding

SUBMISSION DATE / POSTED DATE

07-03-2022 / 11-03-2022

CITATION

Ferguson, Mark; Najah, Mohamed; Banville, Frederic; Boucherit, Mohamed; Gond-Charton, Paul; Renaud, Jacques; et al. (2022): Exploring Ru compatibility with Al-Ge eutectic wafer bonding. TechRxiv. Preprint. https://doi.org/10.36227/techrxiv.19319495.v1

DOI

10.36227/techrxiv.19319495.v1

Exploring Ru compatibility with Al-Ge eutectic wafer bonding

Mark Ferguson, Mohamed Najah, Frederic A. Banville, Mohamed Boucherit, Paul Gond-Charton, Jacques Renaud, Luc Fréchette, François Boone, Serge Ecoffey, Serge A. Charlebois

***Abstract*—We explore compatibility of Ru with Al-Ge eutectic wafer bonding. We first present experiments to check for the presence of Ru ternary alloy poisoning inhibiting Al-Ge melting as well as evaluations of Al-Ge melt wettability on Ru and diffusion outcomes following bond-simulating anneals. Results show that Ru is stable with no observed microstructural changes or dissolution in the melt, indicating no ternary poisoning for the applied thermal budget. Ru was found to act as an effective barrier offering good melt wettability in all considered configurations with Al and Ge. From inspection of the binary constituents of Al-Ge-Ru we propose that Al-Ge eutectic melting temperature will decrease marginally for Ru contamination in a 1-2% range before a drastic increase in melting temperature (>10°C/% Ru) at higher Ru compositions. We then demonstrate wafer-level packaged 200 mm devices and MEMS with strong bond outcomes of devices bearing Ru contacts. We conclude that Ru has high compatibility with Al-Ge eutectic bonding.**

***Index Terms*— aluminium, diffusion barriers, eutectic bonding, germanium, ruthenium, wafer-level packaging**

I. Introduction

EUTECTIC wafer bonding is used in wafer-level packaging (WLP) of devices [1], [2]. Device-bearing wafers set limits on the thermal budget that can be applied by a bonding process, excluding the high temperatures (~1000°C) of direct fusion [3]. Creating reliable MEMS devices generally requires making a hermetic bond against gas and liquid penetration, excluding polymer adhesives [4]. The common requirement of a bonding process that tolerates low planarity disfavors thermocompression bonding [5]. Compatibility with composite metal oxide semiconductor (CMOS) fabrication environments excludes or heavily disfavors materials like Au, as in Au-Sn or Au-Si eutectic bonding [4]. Al-Ge eutectic bonding satisfies these limitations, achieving a strong hermetic bond with CMOS-compatible materials with thermal budgets below 450°C, a ceiling set to avoid the formation of intermetallic species in Al [6].

Ru is a refractory metal used for contact metallization in microelectromechanical systems (MEMS) switches seeking improved reliability [7], [8], [9]. It is a hard material less prone to wear, with a conductive oxide reducing the impact of oxidation on switch resistance. It has been found that mixed soft/hard contacts such as Au/Ru have enhanced stability in contrast to softer (Au/Au) or harder (Ru/Ru) contacts [10]. Most Ru contact studies test unpackaged devices [10], [11], [12]. MEMS device bonding with Al-Ge [13], [14], [15], Au-Sn [16], [17], In-Ga [18] polymer adhesive [7], glass frit and anodic bonding has been reported, but to the best of our knowledge there is a research gap with regard to Ru compatibility with a bonding process. This paper explores the compatibility of Ru in contact with Al-Ge eutectic alloy in the context of a MEMS WLP process.

Concerns about Ru compatibility with Al-Ge bonding are primarily inspired by the case of Si and the need for Si diffusion barriers reported in literature [13], [14], [15]. Si diffusion can introduce melt failure in Al-Ge by the creation of an Al-Ge-Si ternary alloy with an elevated melting temperature. This can be read directly from the Al-Ge-Si phase diagram [19], [20], [21], which bears a eutectic line between the binary eutectic points of Al-Ge at 424°C [13] and Al-Si at ~580°C. Bonding at temperatures too close to the pure Al-Ge eutectic value will therefore be at risk of not melting the layers. References [13] and [14] performed Al-Ge eutectic bonding of MEMS devices, finding a SiO_2 barrier to be necessary to avoid Si ternary formation. Kirkendall voids are observed in literature [22], [23], [24] at Ge/Si or Ge/Al to indicate diffusion at material interfaces, and these can also compromise bond strength. Diffusion barriers can prevent these processes of alloying and voiding, but the wetting of Al-Ge melt to these barriers then becomes a potential problem [24]. An evaluation of Ru compatibility with Al-Ge bonding must then include commentary on the wetting of the Al-Ge melt to Ru and a check for a mechanically-weakened Ru/Al or Ru/Ge interface with voids from interdiffusion with Al and Ge, in addition to resolving the potential ternary alloy poisoning problem.

In this paper, we present an experimental study aimed at demonstrating if Ru poisoning of the Al-Ge eutectic alloy occurs. To do so we perform anneals to simulate the thermal budget of a wafer bonding process. We also comment on wettability of the Al-Ge eutectic melt on Ru underlayers and diffusion at material interfaces with Ru. A qualitative estimation of the metallurgical characteristics that could be expected for an Al-Ge-Ru ternary alloy with a small amount of Ru is developed and presented to justify concern with Ru contamination and suggest a process composition window. Finally, we demonstrate wafer level packaged 200 mm devices and MEMS with strong bond outcomes of devices bearing Ru contacts to further confirm Ru compatibility with Al-Ge eutectic bonding.

II. Materials And Methods

To check for Ru poisoning, wetting and diffusion we consider four stacks of Al, Ge and Ru, deposited as shown in Fig. 1 and identified as Ru-1 through Ru-4. Unlike in a wafer

bonding process, these films are already in good contact favoring material inter-diffusion. Al and Ge layer thicknesses are set at 1 µm and <1 µm respectively. Ru thickness is set to 300 nm, with layer configurations of Ru/Ge/Al, Ru/Al/Ge and Al/Ru/Ge for the first 3 stacks. Ru contaminates Ge and Al respectively in Ru-1 and Ru-2, and serves as a diffusion barrier in Ru-3. For device-bearing wafers with Ru patterning on Al we confirmed Ru contamination of the Al surface via energy dispersive X-ray spectroscopy (EDS). A device-bearing wafer with this Ru-contaminated Al was subjected to a blanket deposition of Ge followed by the same bond-simulating anneal to look for impaired melting. Such samples are dubbed Ru-4.

These stacks were annealed as 1 cm × 1 cm samples. The thermal profile chosen was a gradual ramp of 8 minutes to a temperature above 424°C, a maximum temperature then held for 30 minutes, a customized thermal profile corresponding to the profiles used in Al-Ge bonding [13], [14]. Flowing nitrogen was used to exclude oxygen and moisture from the chamber.

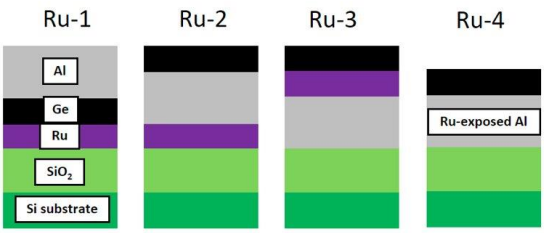

Fig. 1. Layered structures of samples Ru-1, Ru-2, Ru-3 and Ru-4 for full-area contact anneal experiments. Thicknesses are <1000 nm (Ge), 1000 nm (Al), 300 nm (Ru) and 2000 nm (SiO_2).

After annealing the wafers were cleaved to allow for examination of layer cross-sections by scanning electron microscopy (SEM) to differentiate cases of melted and unmelted Al/Ge layers. Surveys of >30 µm were made of each cross-section. As a precautionary check we performed a similar set of experiments on multilayers of Si, Al and Ge, for which Si poisoning of Al-Ge eutectic is known. This is reported in the Appendix.

As a final demonstration, wafer level packaged MEMS were fabricated on 200 mm wafers with Ru-bearing device wafers. The quality of the bond was inspected and qualified by infrared (IR) transmission microscopy with the McBain DDR200 NIR tool, by diamond blade dicing to singulate the different cells, and by destructive mechanical deprocessing of multiple singulated MEMS to examine the breakage interface.

III. Results and Discussion

A. *Blanket depositions annealing outcomes*

To the knowledge of these authors, potential Ru interference with Al-Ge bond outcome has not been published, but commentary can now be given.

A search for binary Al-Ge melt poisoning by Ru and poor wetting in SEM cross-sections (Fig. 2) finds no evidence of either problem. Cases Ru-1 and Ru-2 both show successful full melting of the Al-Ge layers despite close contact with Ru. The Ru/melt interface is continuous in all observations, indicating good wetting. The as-deposited Al layer had high uniformity in thickness, but melt thickness variation over the Ru layer post-anneal is high, from below 1 to >3 µm, indicating flow and migration of material, likely due to surface tension.

Ru diffusion barrier effectiveness is evaluated in case Ru-3. No eutectic is observed, with an intact layer of Ru serving as an effective barrier against Al-Ge interdiffusion. All layers in contact with Ru in all cross-sections do not undergo any obvious evolution. We observe no Kirkendall voids, suggesting minimal interdiffusion of Ru with Al or Ge, with any diffusion expected to eventually produce such voids. These results are contrasted with Si diffusion and wetting outcomes presented in the Appendix.

With the applied thermal budget Ru compatibility with bonding is high. However, as elements diffuse and compete to form alloys it should be noted that they will not always compete on equal footing: although Ge/Si interdiffusion is also not competitive with Ge diffusion into Al [25], [26] the slower process can compete when it starts before Ge exposure to Al. It is then possible to imagine scenarios where Ru becomes competitive and inhibitory for bonding due to earlier diffusion. Therefore, Ru etching needs careful optimization [27] such that contamination is minimized to prevent poisoning of Al-Ge melts.

In developing devices for Al-Ge bonding, Ru-exposed Al was inspected. EDS examination of the Al surfaces showed a Ru trace signal confirming contamination. Al and Ru are in contact for multiple thermal cycles associated with Ru patterning prior to the bonding step, giving opportunity for diffusion. A blanket deposition of Ge on this Ru-exposed Al was annealed to investigate if the confirmed Ru contamination affects the melt of Al-Ge. We observed no manifestations of melt impairment in cross-sections after annealing, comparable to Ru-1 and Ru-2.

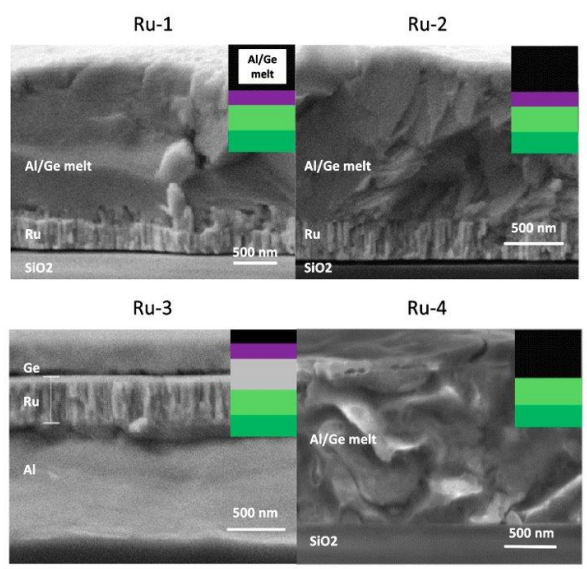

Fig. 2. Post-anneal samples examined by SEM cross-sectioning. a-b) Case Ru-1 (Ru/Ge/Al) and Case Ru-2 (Ru/Al/Ge) show successful eutectic melt proceeding down to the Ru layer, with good adhesion to the Ru. c) Case Ru-3 (Al/Ru/Ge) show Ru serving as an effective diffusion barrier, not interacting with either species. d) Case Ru-4 with Ru-exposed Al, showing successful eutectic melt despite some Ru

contamination.

B. A qualitative description of the Ru composition process window for Al-Ge eutectic bonding

To the best of our knowledge the Al-Ge-Ru ternary phase diagram has not been mapped. Multiple models exist to approach the task of interpolating ternary phase diagrams from binary systems by CALPHAD (calculation of phase diagrams) [28]. But when the difference in melting point and other properties between elements is significant extrapolations become unreliable and need experimental validation [29]. Modeling Ru as a component with Al and Ge would have this difficulty because of the large difference in melting point (>1000°C). Ru penetration into Al has been directly measured [30], with Ru solubility in Al reported to be negligible [31] or difficult [32]. Ru diffusion into Ge has been described as not noticeable [33], and comparable impurities are known to have low solubility in Ge [34]. These facts justify a focus on the low-Ru region of the ternary, where a eutectic line terminates at the Al-Ge binary eutectic point at 424°C.

From references [32], [35], [36], [37] we extract the slope of the liquidus temperature with increasing Ru content in the Ru-X binaries for a small addition of Ru to Al and Ge. Both Al-Ru and Ge-Ru have a low-Ru eutectic point and the slopes are evaluated for Ru compositions above these points. For Al-Ru a eutectic point exists at ~1% with a 3°C reduction in melting temperature from pure Al, and the liquidus slope for higher Ru compositions is ~75°C/% Ru. For Ge-Ru a eutectic point exists at ~2% with a ~11°C reduction in melting temperature from pure Ge, and the liquidus slope for higher Ru compositions is ~54°C/% Ru. It is thus reasonable to believe that Ru could increase the melting temperature of the poisoned Al-Ge significantly above its nominal 424°C value. We therefore expect a narrow Ru-contamination allowed range for Al-Ge eutectic formation in the process window below 450°C. This behavior is summarized in Fig. 3.

Until Al-Ge-Ru is mapped like Al-Ge-Si, the validity of this description is an open question. Small features in the binaries are still prone to disagreement and re-evaluation [38], and available ternaries with Al and Ru may have many complex and discontinuous local features in their eutectic lines [39], or leave extreme compositions unexplored [40], [41], [42], [43]. The lack of microstructural changes such as Kirkendall voids at interfaces with Ru suggest that significant diffusion is not occurring, and Ru has been deemed stable enough to use as a diffusion barrier for Cu in some applications [44]. The fact that we observe good melting in Ru-1, Ru-2 and Ru-4 is compatible with this qualitative description and gives confidence to the suggestion that deep interpolations into the ternary are not very relevant for wafer bonding applications. Challenges in an Al-Ge bonding process from Ru are unlikely to have a metallurgical explanation. To complement the bonding compatibility picture from the blanket anneals, the wettability assessment was shown to be excellent. Our analysis is supported by contrasting our observations of Si poisoning of Al-Ge described in the Appendix.

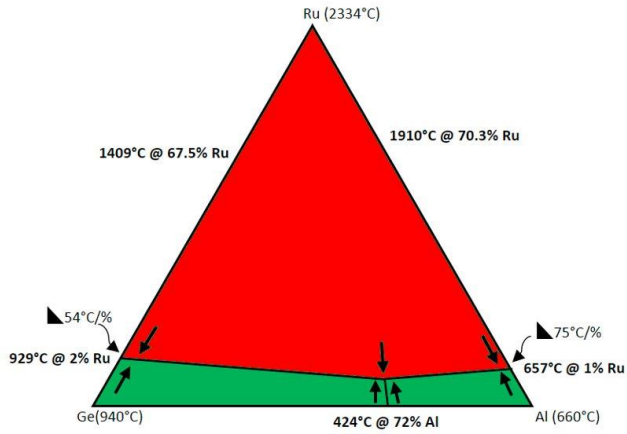

Fig. 3. Qualitative description of composition process window for Al-Ge eutectic melting in the presence of Ru, depicted on a frame of the Al-Ge-Ru ternary phase diagram. Pure element melting points indicated at corners, binary eutectic point temperatures/compositions indicated at edges in bold text, Ru sensitivity slopes for Al-Ru and Ge-Ru binaries in low-Ru region indicated with right-angled triangles. All fractions molar and axes not to scale for legibility. Melting temperatures of Al-Ge alloys are expected to decrease marginally in low composition range (green zone) before high sensitivity to Ru composition elevates melting temperature (red zone). Eutectic lines converging to a ternary point with one line terminating at the Al-Ge binary eutectic point indicated, with black arrows indicating descending melting temperature.

C. Bonded device-bearing wafers

As a demonstration of Ru compatibility with Al-Ge wafer bonding, strong bonds were achieved in a 200 mm wafer MEMS process that includes Ru contacts. Continuous seal rings were observed in infrared transmission microscopy with a McBain DDR200 NIR tool (Fig. 4a). These bonded devices furthermore survived dicing to singulate cells. Destructive debonding of singulated cells by knife edge showed extensive transfer of torn Si to the device along the seal ring, indicating high bond strength (Fig 4b).

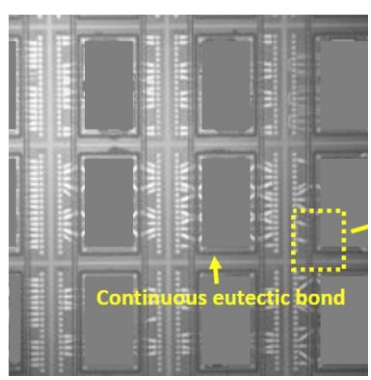

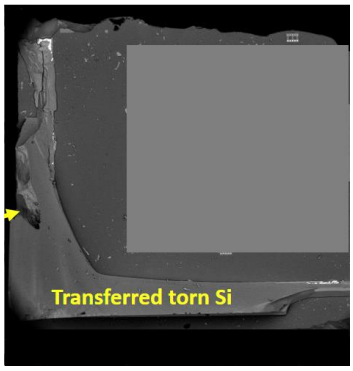

(a) (b)

Fig. 4. Wafer bond inspection for Ru-contact devices: a) IR transmission microscopy, imaging continuous seal rings; b) SEM image of singulated, destructively-debonded cell showing torn Si transferred to the device side at seal ring.

IV. Conclusion

We have investigated the influence of Ru contamination in Al-Ge eutectic bonding, which is extensively used in the MEMS fabrication process. The strong impact on melting temperature from Ru content in Al-Ru and Ge-Ru binaries raises concerns of a detrimental role for Ru in Al-Ge bonding. Using stacked blanket layers of Al, Ge and Ru in several arrangements we were able to confirm 1) proper formation of Al-Ge melts in both Ru/Al/Ge and Ru/Ge/Al stacks, 2) good wetting for Al-Ge eutectic melt on Ru, and 3) the performance of Ru as a diffusion barrier in a Al/Ru/Ge stack. No Kirkendall voids were observed at any Ru interfaces, suggesting very low diffusion of Ru into the other species. From inspection of the binary constituents of Al-Ge-Ru we propose that Al-Ge eutectic melting temperature will decrease marginally for Ru contamination in a 1-2% range before a drastic increase in melting temperature (>10°C/% Ru) at higher Ru compositions. Finally, 200 mm wafers bearing MEMS devices with Ru contacts were successfully fabricated using Al-Ge eutectic bonding, with strong bonds confirmed in destructive deprocessing.

Appendix

Si diffusion is known to significantly interfere with the formation of Al-Ge eutectic. To validate our experimental approach regarding Ru we performed similar annealing experiments with stacks of Al, Ge and Si without and with diffusion barriers of SiO_2 and TiW, depicted in Fig. 5. Layer stacks were deposited with HF cleaning of Ge prior to Al deposition to prevent interference by intermediate oxides.

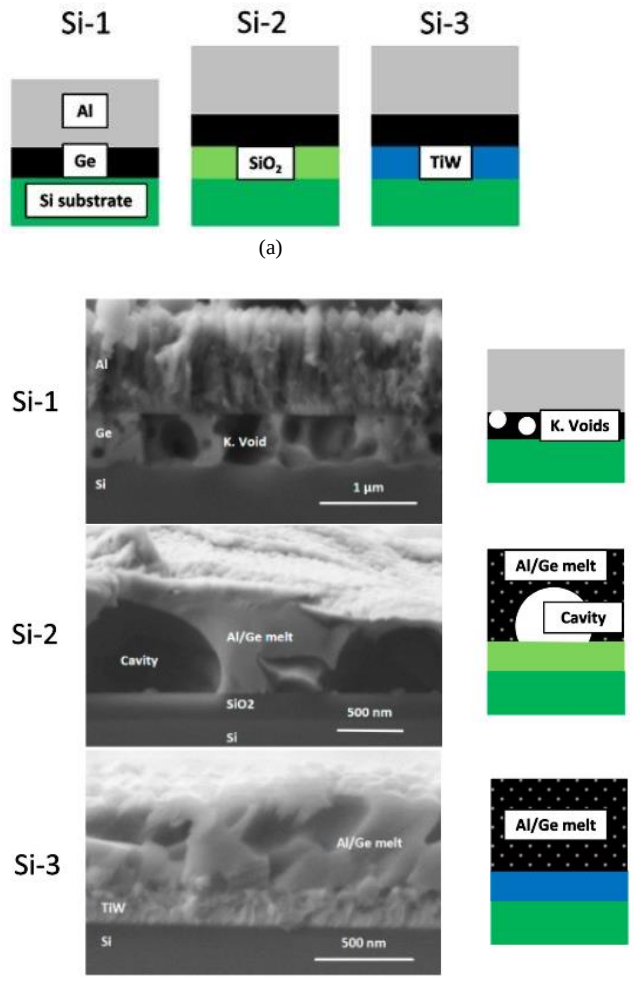

Fig. 5. Si impact on Al-Ge verification. a) layered structure of samples Si-1, Si-2 and Si-3 for Si poisoning confirmation and diffusion barrier evaluation. Thicknesses are <1000 nm (Ge), 1000 nm (Al), 200 nm (SiO_2) and 200 nm (TiW). b) Post-anneal samples examined by SEM cross-sectioning. Al-Ge melt inhibition is clearly observed (top) with well-defined layers and Kirkendall voids at the Si/Ge interface. With a SiO_2 diffusion barrier Al-Ge melt forms (middle) but does not properly wet the barrier. Proper melt and wetting behavior on TiW (bottom).

After annealing, Si-1 has two distinct layers of the original thicknesses, indicating a failure of the Ge and Al to make a eutectic despite good contact, heating and removal of Ge oxide before Al deposition. The bottom layer of Ge features significant Kirkendall voids, indicating Ge/Si interdiffusion and Ge loss to the substrate. Case Si-2 shows eutectic melt on top of the SiO_2 diffusion barrier, with no differentiable Ge and Al layers; notably, the melt's wetting of the oxide barrier is poor, resulting in large cavities in the melt. In contrast, a successful eutectic formed on top of the TiW diffusion barrier of Si-3 with good adhesion to the barrier and no interface voids. Both barriers have blocked Si diffusion to allow full Al-Ge melting. These wettability results are compatible with a reference[24], who found Al-Ge melt wetting on SiO_2 to be inferior to TiN.

ACKNOWLEDGMENTS

This work was supported by the Natural Sciences and Engineering Research Council (NSERC), by the Mitacs organization, by Prompt (a member of the QuébecInnove organization), and by Teledyne DALSA (TDSI).Special acknowledgements are given to TDSI for their continuous support and guidance, to Stéphane Morin and Caroline Roy of the Interdisciplinary Institute for Technological Innovation (3IT) for assistance in depositions, and to Professor Raafat Mansour, Tejinder Singh, Ahmed Aziz and Jaouad Marzouk of the Centre for Integrated RF Engineering (CIRFE) for designs and advisement on RF MEMS.

REFERENCES

[1] T. Ye, Z. Song, Y. Du, Z. Wang, "Reliability of Au-Si eutectic bonding," presented at the ICEPT15, Chengdu, China, October 2014, pp. 1080-1082, doi: 10.1109/ICEPT.2014.6922833.

[2] W. Reinert, A. Kulkarni, V. Vuorinen, P. Merz, "Metallic Alloy Seal Bonding," in *Handbook of Silicon Based MEMS Materials and Technologies*, 2nd ed., Elsevier, 2015, pp. 626–639.

[3] C.T. Ko, K.N. Chen, "Wafer-level bonding/stacking technology for 3D integration," *Microelectron. Reliab*., vol. 50, iss. 4, pp. 481-488, April 2010, doi: 10.1016/j.microrel.2009.09.015.

[4] S. Sood. "Advanced Metal-Eutectic Bonding for High Volume MEMS WLP," presented at the IEEE MEMS 2014, San Francisco, CA, USA, Feb. 2014.

[5] C.H. Tsau, S.M. Spearing, M.A. Schmidt, 'Fabrication of Wafer-Level Thermocompression Bonds,' *J. Microelectromech. Syst*., vol. 11, no. 6, pp. 641-647, December 2002, doi: 10.1109/JMEMS.2002.805214.

[6] V.N. Danilenko, S.N. Sergeev, J.A. Baimova, G.F. Korznikova, K.S. Nazarov, R.Kh. Khisamov, A.M. Glezer, R.R. Mulyukov, "An approach for fabrication of Al-Cu composite by high pressure torsion," *Mater. Lett.*, vol. 236, pp. 51-55, 2019, doi: 10.1016/j.matlet.2018.09.158

[7] F. Ke, J. Miao, J. Oberhammer, "A Ruthenium-Based Multimetal-Contact RF MEMS Switch with a Corrugated Diaphragm," *J. Microelectromech. Syst.*, vol. 17, no. 6, pp. 1447–1459, Dec. 2008, doi: 10.1109/JMEMS.2008.2004786.

[8] A. Basu, R. Hennessy, G. Adams, N. McGruer, "Reliability in Hot Switched Ruthenium on Ruthenium MEMS Contacts," presented at the IEEE Holm Conference on Electrical Contacts, Newport, RI, USA, Sep. 2013, pp. 1–8, doi: 10.1109/HOLM.2013.6651422.

[9] S. M. Karabanov, A.S. Karabanov, D.V. Suvorov, B. Grappe, C. Coutier, H. Sibuet, B.N. Sazhin, "Magnetically controlled MEMS switches with nanoscale contact coatings," presented at ICEC 2012, Beijing, China, 2012, pp. 359–361, doi: 10.1049/cp.2012.0675.

[10] A. Broué, J. Dhennin, F. Courtade, C. Dieppedale, P. Pons, X. Lafontan, R. Plana, "Characterization of gold/gold, gold/ruthenium, and ruthenium/ruthenium ohmic contacts in MEMS switches improved by a novel methodology," *Proc. SPIE*, vol. 7592, pp. 75920A-1-75920A-12, Feb. 2010.

[11] C.D. Patel, G.M. Rebeiz, "An RF-MEMS Switch with mN Contact Forces," presented at the IEEE MTT-S 2010, Anaheim, CA, USA, pp. 1242-1245, May 2010, doi: 10.1109/MWSYM.2010.5517237.

[12] W.M. van Spengen, "Capacitive RF MEMS switch dielectric charging and reliability: a critical review with recommendations," *J. Micromech. Microeng.*, vol. 22, no. 7, pp. 1-23, 2012, doi: 10.1088/0960-1317/22/7/074001.

[13] F. Crnogorac, R. Birringer, R. Dauskardt, F. Pease, "Aluminum-Germanium eutectic bonding for 3D integration," presented at 3DIC 2009, San Francisco, CA, USA, Sep. 2009, pp. 1–5, doi: 10.1109/3DIC.2009.5306531.

[14] F. Crnogorac, F. Pease, R. Birringer, R. Dauskardt, "Low-temperature Al–Ge bonding for 3D integration," *J. Vac. Sci. Technol. B.*, vol. 30, no. 6, p. 06FK01, Nov. 2012, doi: 10.1116/1.4762844.

[15] W.T. Park, J.W. Jang, T. Clare, L. Liu, "Microstructure and mechanical properties of aluminum-germanium eutectic bonding with polysilicon metallization for microelectromechanical systems (MEMS) packaging," *Scr. Mater.*, vol. 64, iss. 8, pp. 733-736, April 2011, doi: 10.1016/j.scriptamat.2010.12.024.

[16] D.A. Czaplewski, C.D. Nordquist, G.A. Patrizi, G.M. Kraus, W.D. Cowan, "RF MEMS Switches With RuO2-Au Contacts Cycled to 10 Billion Cycles," *J. Microelectromech. Syst.*, vol. 22, no. 3, pp. 655-661, June 2013, doi: 10.1109/JMEMS.2013.2239256.

[17] J.H. Park, H.C. Lee, Y.H. Park, Y.D. Kim, C.H. Ji, J.Bu, H.J. Nam, "A fully wafer-level packaged RF MEMS switch with low actuation voltage using a piezoelectric actuator," *J. Micromech. Microeng.*, vol. 16, no. 11, pp. 2281-2286, September 2006, doi: 10.1088/0960-1317/16/11/005

[18] B.F. Toler, R.A. Coutu Jr, J.W. McBride, "A review of micro-contact physics for microelectromechanical systems (MEMS) metal contact switches," *J. Micromech. Microeng.*, vol. 23, no. 10, pp. 103001, September 2013, doi: 10.1088/0960-1317/23/10/103001.

[19] H. Song and A. Hellawell, "Solidification in the System Al-Ge-Si: The Phase Diagram, Coring Patterns, Eutectic Growth, and Modification," *Metallurgical Trans. A*, vol. 21, pp. 733-740, March. 1990, doi: 10.1007/BF02671944.

[20] F.H. Hayes, R.D. Longbottom, E. Ahmad, G. Chen, "On the Al-Si, Al-Ge, and Al-Ge-Si Systems and Their Application to Brazing in High Power Semiconductor Devices," *J. Phase Equilib.*, vol. 14, no. 4, pp. 425-431, 1993, doi: 10.1007/BF02671960.

[21] V.N. Gurin, S.P. Nikanorov, M.P. Volkov, L.I. Derkachenko, T.B. Popova, I.V. Korkin, B.R. Willcox, L.L. Regel, "Crystallization in the Al-Si, Al-Ge, and Al-Si-Ge systems at centrifugation," *Tech. Phys.*, vol. 50, no. 3, pp. 341-346, 2005, doi: 10.1134/1.1884734.

[22] E. S. Marstein, A.E. Gunnæs, U. Serincan, S. Jørgensen, A. Olsen, R. Turan, T.G. Finstad, "Mechanisms of void formation in Ge implanted SiO2 films," *Nucl. Instrum. Methods Phys. Res. Sect. B*, vol. 207, no. 4, pp. 424–433, Aug. 2003, doi: 10.1016/S0168-583X(03)00965-0.

[23] V. Sivadasan, S. Rhead, D. Leadley, M. Myronov, "Kirkendall void formation in reverse step graded Si1-xGex /Ge/Si (001) substrates," *Semicond. Sci. Technol.*, vol. 33, no. 2, pp. 024002, January 2018, doi: 10.1088/1361-6641/aaa329.

[24] V. Lumineau, F. Fournel, B. Imbert, F. Hodaj, "Aluminum-Germanium eutectic bonding for MEMS: behaviour and solidification of liquid Al-Ge on different substrates," *ECS Trans.*, vol. 75, no. 9, pp. 273-281, 2016, doi: 10.1149/07509.0273.

[25] E. Ganniari-Papageorgiou, M. E. Fitzpatrick, and A. Chroneos, "Germanium diffusion in aluminium: connection between point defect parameters with bulk properties," *J. Mater. Sci. Mater. Electron.*, vol. 26, no. 11, pp. 8421–8424, Nov. 2015, doi: 10.1007/s10854-015-3510-5.

[26] M. Gavelle, E.M. Bazizi, E. Scheid, P. F. Fazzini, F. Cristiano, C. Armand, W. Lerch, S. Paul, Y. Campidelli, A. Halimaoui, "Detailed investigation of Ge-Si interdiffusion in the full range of Si1-xGex($0 \leq x \leq 1$) composition," *J. Appl. Phys.*, vol. 104, no. 11, pp. 113524, 2008, doi: 10.1063/1.3033378.

[27] M. Najah, M. Ferguson, M. Boucherit, M. Guilmain, J. Renaud, L. Fréchette, S. Charlebois, F. Boone, S. Ecoffey, "Ru plasma etching process for thermally stable and low resistivity contacts", presented at MNE 2021, Torino, Italy, September 20 - 23, 2021.

[28] A.D. Pelton, "A General "Geometric" Thermodynamic Model for Multicomponent Solutions," *Calphad*, vol. 25, iss. 2, pp. 319-328, 2001, doi: 10.1016/S0364-5916(01)00052-9.

[29] Q. Luo, C. Zhai, D. Sun, W. Chen, Q. Li, "Interpolation and extrapolation with the CALPHAD method," *J. Mat. Sci. Technol*, vol. 35, iss. 9, pp. 2115-2120, 2019, doi: 10.1016/j.jmst.2019.05.016.

[30] F. Dyment, S. Balart, C. Lugo, R. A. Pérez, N. Di Lalla, M. J. Iribarren, "Ru Self-Diffusion and Ru Diffusion in Al," *Def. Diffus. Forum*, vol. 237–240, pp. 402–407, Apr. 2005, doi: 10.4028/www.scientific.net/DDF.237-240.402.
[31] S.N. Prins, L.A. Cornish, W.E. Stumpf, B. Sundman, "Thermodynamic Assessment of the Al-Ru System," *Calphad*, vol. 27, no.1, pp. 79-90, 2003, doi: 10.1016/S0364-5916(03)00033-6.
[32] S. Mi, S. Balanetskyy, B. Grushko, "A study of the Al-rich part of the Al–Ru alloy system," *Intermetallics*, vol. 11, p. 643-649, 2003, doi: 10.1016/S0966-9795(03)00052-9.
[33] L. Perring, P. Feschotte, J.C. Gachon, "The germanium-ruthenium system," *J. Phase Equilib.*, vol. 17, pp. 101-106, 1996, doi: 10.1007/BF02665783
[34] C. Claeys and E. Simoen, "Diffusion and Solubility of Dopants in Germanium," in *Germanium-Based Technologies: From Materials to Devices*, 1st ed., Elsevier, 2007, pp. 67-96.
[35] A.D. Pelton, C. Bale, "SGTE - SGTE 2017 Alloy Phase Diagrams (1176)", FactSage 8.1 - Summary of Databases, Sept. 21, 2021. [Online]. Available: http://www.crct.polymtl.ca/fact/documentation//SGTE2017/SGTE2017_Figs.htm
[36] F. Mücklich and N. Ilić, "RuAl and its alloys. Part I. Structure, physical properties, microstructure and processing," *Intermetallics*, vol. 13, no. 1, pp. 5–21, Jan. 2005, doi: 10.1016/j.intermet.2004.05.005.
[37] Z. H. Long, H. S. Liu, Z. P. Jin, "Thermodynamic description of Ru–Ge–Si ternary system," *J. Alloys Compd.*, vol. 479, pp. 262-267, 2009, doi: 10.1016/j.jallcom.2009.01.079.
[38] H. Okamoto, 'Al-Ru (Aluminum-Ruthenium)', *J. Phase Equilib. Diffus.*; Materials Parks, vol. 27, iss. 4, pp. 426, 2006, doi: 10.1361/154770306X116504.
[39] V. Raghavan, 'Al-Pt-Ru (Aluminum-Platinum-Ruthenium)', *J. Phase Equilib. Diffus.*, vol. 32, no. 6, pp. 564-565, 2011, doi: 10.1007/s11669-011-9945-3.
[40] V. Raghavan, 'Al-Ir-Ru (Aluminum-Iridium-Ruthenium)', *J. Phase Equilib. Diffus.*, vol. 31, no. 3, pp. 291-292, 2003, doi: 10.1007/s11669-010-9683-y.
[41] V. Raghavan, 'Al-Cu-Ru (Aluminum-Copper-Ruthenium)', *J. Phase Equilib. Diffus.*, vol. 27, no. 2, pp. 153-155, 2006, doi: 10.1361/154770306X97227.
[42] V. Raghavan, 'Al-Ni-Ru (Aluminum-Nickel-Ruthenium)', *J. Phase Equilib. Diffus.*, vol. 27, no. 5, pp. 501-504, 2006, doi: 10.1361/154770306X136412.
[43] V. Raghavan, 'Al-Cr-Ru (Aluminum-Chromium-Ruthenium)', *J. Phase Equilib. Diffus.*, vol. 32, no. 5, pp. 451, 2011, doi: 10.1007/s11669-011-9919-5.
[44] D.C. Perng, K.C. Hsu, S.W. Tsai, J.B. Yeh, "Thermal and electrical properties of PVD Ru (P) film as a Cu diffusion barrier," *Microelectron. Eng.*, vol. 87, no. 3, pp. 365-369, 2010, doi: 10.1016/j.mee.2009.06.007.

Figures and captions:

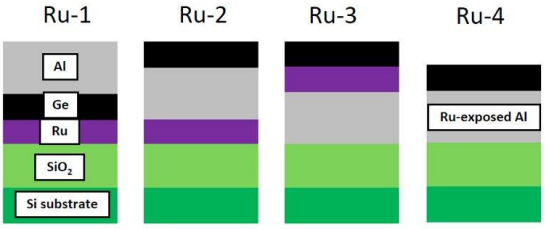

Fig. 1. Ru impact variations Ru-1, Ru-2, Ru-3 and Ru-4 for full-area contact anneal experiments. Thicknesses are <1000 nm (Ge), 1000 nm (Al), 300 nm (Ru) and 2000 nm (SiO_2).

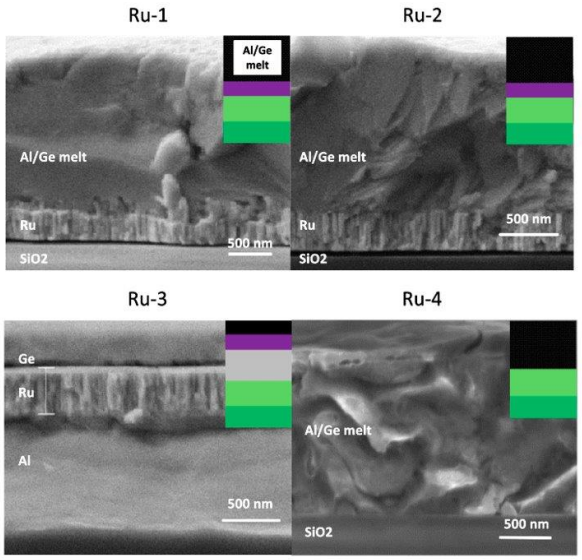

Fig. 2. Post-anneal samples examining Ru impact on the Al-Ge eutectic, examined by SEM cross-sectioning. a-b) Case Ru-1 (Ru/Ge/Al) and Case Ru-2 (Ru/Al/Ge) show successful eutectic melt proceeding down to the Ru layer, with good adhesion to the Ru. c) Case Ru-3 (Al/Ru/Ge) show Ru serving as an effective diffusion barrier, not interacting with either species. d) Case Ru-4 with Ru-exposed Al, showing successful eutectic melt despite some Ru contamination.

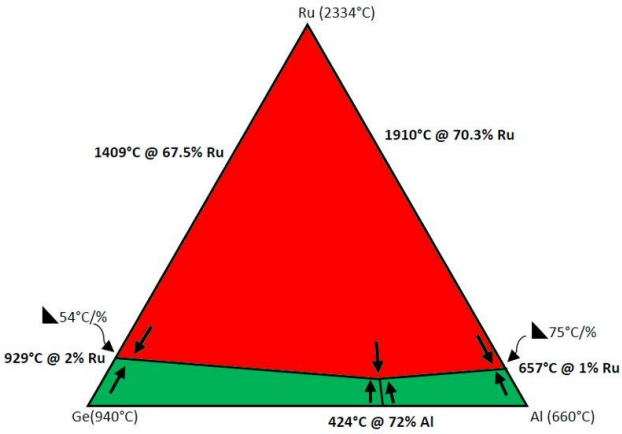

Fig. 3. Qualitative description of composition process window for Al-Ge eutectic melting in the presence of Ru, depicted on a frame of the Al-Ge-Ru ternary phase diagram. Pure element melting points indicated at corners, binary eutectic point temperatures/compositions indicated at edges in bold text, Ru sensitivity slopes for Al-Ru and Ge-Ru binaries in low-Ru region indicated with right-angled triangles. All fractions molar and axes not to scale for legibility. Melting temperatures of Al-Ge alloys are expected to decrease marginally in low composition range (green zone) before high sensitivity to Ru composition elevates melting temperature (red zone). Eutectic lines converging to a ternary point with one line terminating at the Al-Ge binary eutectic point indicated, with black arrows indicating descending melting temperature.

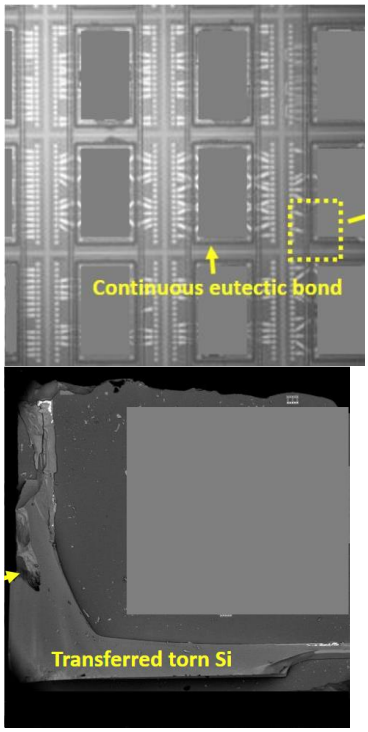

(a) (b)

Fig. 4. Wafer bond inspection for Ru-contact devices: a) IR transmission microscopy, imaging continuous seal rings; b) SEM image of singulated, destructively-debonded cell showing torn Si transferred to the device side at seal ring.

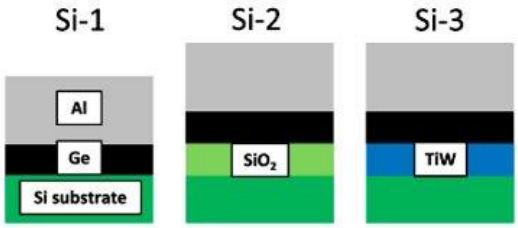

(a)

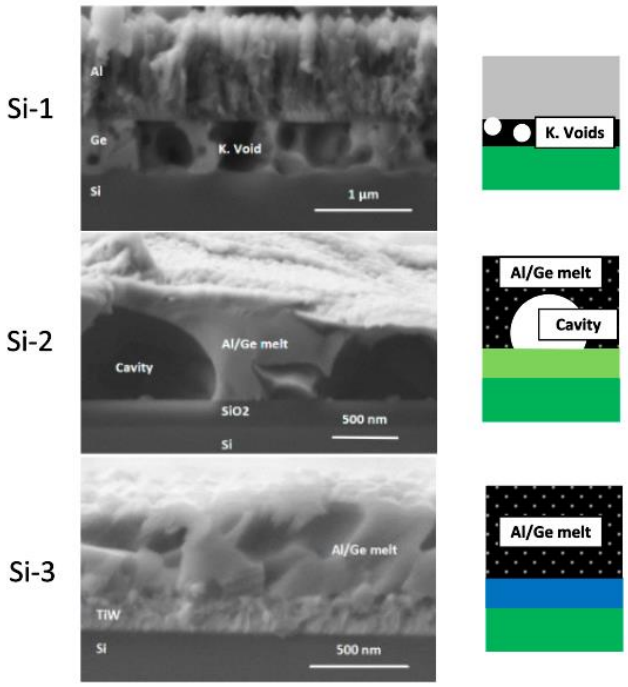

(b)

Fig. 5. Si impact on Al-Ge verification. a) layered structure of samples Si-1, Si-2 and Si-3 for Si poisoning confirmation and diffusion barrier evaluation. Thicknesses are <1000 nm (Ge), 1000 nm (Al), 200 nm (SiO_2) and 200 nm (TiW). b) Post-anneal samples examined by SEM cross-sectioning. Al-Ge melt inhibition is clearly observed (top) with well-defined layers and Kirkendall voids at the Si/Ge interface. With a SiO2 diffusion barrier Al-Ge melt forms (middle) but does not properly wet the barrier. Proper melt and wetting behavior on TiW (bottom).